FULL PAPER

Dalton
www.rsc.org/dalton

Formation of heterotopic metallacalix[*n*]arenes (*n* = 3, 4, 6) containing ethylenediaminepalladium(II) metal fragments and 4,7-phenanthroline and 2-pyrimidinolate bridges. Synthesis, structure and host–guest chemistry

Miguel A. Galindo,[a] Simona Galli,[b] Jorge A. R. Navarro*[a] and M. Angustias Romero*[a]

[a] *Departamento de Química Inorgánica, Universidad de Granada, Av. Fuentenueva S/N, E-18071 Granada, Spain. E-mail: jarn@ugr.es; maromero@ugr.es; miangel@ugr.es; Fax: (+34)958248526*

[b] *Dipartimento di Scienze Chimiche ed Ambientali, Università degli Studi dell'Insubria, via Valleggio 11, I-22100 Como, Italy. E-mail: simona.galli@uninsubria.it*

Received 9th June 2004, Accepted 6th July 2004
First published as an Advance Article on the web 3rd August 2004

A multicomponent reaction involving ethylenediaminepalladium(II), 2-pyrimidinol derivatives (L) [L = 2-pyrimidinol (**a**); 4-methyl-2-pyrimidinol (**b**); 4,6-dimethyl-2-pyrimidinol (**c**)] and 4,7-phenanthroline (4,7-phen) leads to the formation of heterotopic cyclic metallamacrocycles of the type $[Pd_n(en)_n(\mu\text{-}N,N'\text{-}L)_m(\mu\text{-}N,N'\text{-}4,7\text{-}phen)_{n-m}]^{(2n-m)+}$ [$n = 3$, $m = 1$ (**3**); $n = 4$, $m = 2$ (**4**); $n = 6$, $m = 4$ (**5**)]. These species can be obtained by different reaction pathways, including: (i) reaction of ethylene diaminepalladium(II), L and 4,7-phen building blocks and (ii) reaction of the homotopic species $[Pd_4(en)_4(\mu\text{-}N,N'\text{-}L)_4]^{4+}$ (**1**) and $[Pd_3(en)_3(\mu\text{-}N,N'\text{-}4,7\text{-}phen)_3]^{6+}$ (**2**). The resulting heterotopic metallamacrocycles have been characterised by 1D and 2D ^{1}H NMR spectroscopy. Additionally, species **3c** and **4a** have been studied by X-ray crystallography. The former one contains almost isosceles triangles of $[Pd_3(en)_3(\mu\text{-}N,N'\text{-}4,6\text{-dimethyl-2-pyrimidinolate})(\mu\text{-}N,N'\text{-}4,7\text{-phen})_2]^{5+}$ formulation, exhibiting a pinched-cone conformation. **4a** contains a tetranuclear parallelogram $[Pd_4(en)_4(\mu\text{-}N,N'\text{-2-pyrimidinolate})_2(\mu\text{-}N,N'\text{-}4,7\text{-phenanthroline})_2]^{6+}$, exhibiting a 1,3-alternate conformation. The host–guest properties of the here reported species have been studied, showing that they are able to interact with cationic as well as with anionic species.

Introduction

Organic synthesis of complex molecular architectures normally implies the use of protecting groups and multiple reaction steps, tedious separations and low yields. Such inconveniences can be overcome by employing self-assembly processes involving metal ions and organic ligands of suitable geometry to build multicomponent complex molecular architectures in a single step.[1,2] Selection of a target product can be made by the convenient choice of metal fragment and ligand geometries, as well as the presence of templating agents[3] or ligand functionalization.[4] Small-protein-sized molecules have been synthesized in this way,[3] and there are numerous reports on exciting host–guest chemistry of such systems and interesting applications relevant to sensing and selective catalytic reactions in the confined space of a capsule.[5]

Others and ourselves have previously shown the suitability of combining protected metal ions and N-heterocycles providing bent bond angles to build metal analogues of calix[*n*]arenes with $n = 3$,[6–8] 4,[9] 6.[10,11] In this context, we have proven that reaction of the ethylenediaminepalladium(II) metal fragment with 2-pyrimidinol (2-Hpymo) or its methylated derivative 4,6-dimethyl-2-pyrimidinol (2-Hdmpymo) quantitatively yields tetranuclear metallacalix[4]arenes of the type $[Pd(en)(\mu\text{-}N,N'\text{-2-pymo})]_4^{4+}$ (**1**).[9c,d] With a similar approach, Yu *et al.*[6] employed 4,7-phenanthroline (4,7-phen) to build a metal analogue of calix[3]arene of the $[Pd(en)(\mu\text{-}N,N'\text{-}4,7\text{-phen})]_3^{6+}$ type (**2**).

The similar geometric requirements of 2-pyrimidinol derivatives and 4,7-phenanthroline prompted us to explore the possible formation of heterotopic metallamacrocycles containing these two types of *N*,*N*′-*exo*-bidentate ligands with the concomitant possibility of engineering the shape and size of these species. Thus, in this manuscript, we report a multicomponent reaction involving *cis*-protected palladium(II) metal fragments, 2-pyrimidinol derivatives and 4,7-phenanthroline. Such a complex reaction mixture can lead to the formation of a wide variety of species, such the novel heterotopic trinuclear (**3**), tetranuclear (**4**) and hexanuclear (**5**) species depicted in Scheme 1. However, depending on reaction conditions, stoichiometry and pyrimidine functionalisation, selection of a specific product can be made.

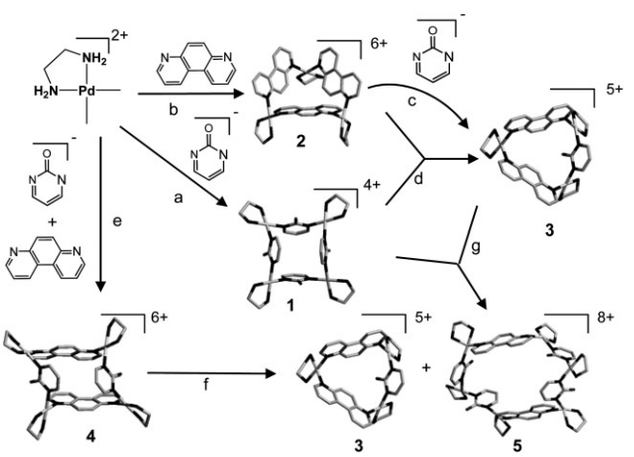

Scheme 1 Summary of the cyclic species that can be obtained containing ethylenediaminepalladium(II), 4,7-phen and 2-pymo derivatives. $R_{1,2}$ = H, CH_3. (a) Ref. 9(*d*),(*e*); (b) ref. 6; (c) **2** + 2-pymo, 2 h at 60 °C, gives **3** + free 4,7-phen; (d) a 3 : 8 mixture of **1** and **2**, for 2 h at 80 °C, gives **3** (12 equivalents); (e) $enPd^{II}$ + 2-pymo + 4,7-phen, in the ratio 4 : 2 : 2, for 24 h at 80 °C, give **4**; (f) **4**, 24 h at 80 °C, gives a 2 : 1 mixture of **3** and **5**; (g) **1** + **3** (excess), 24 h at 80 °C, gives **5** + unreacted **3**.

Results and discussion

Trinuclear species of type $[Pd_3(en)_3(\mu\text{-}N,N'\text{-L})(\mu\text{-}N,N'\text{-}4,7\text{-phen})_2]^{5+}$ (3)

The simplest heterotopic species of this series, of $[Pd_3(en)_3(\mu\text{-}N,N'\text{-L})(\mu\text{-}N,N'\text{-}4,7\text{-phen})_2]^{5+}$ type [L = 2-pymo (**3a**); 4-methyl-2-pymo (**3b**); 4,6-dimethyl-2-pymo (**3c**)], can be obtained by three different reaction pathways, irrespectively of the pyrimidine ring functionalisation: (i) by direct reaction from a 3 : 1 : 2 mixture of ethylenediaminepalladium(II), L and 4,7-phen building blocks (not included

DOI: 10.1039/b408698h

in Scheme 1); (ii) by ligand exchange of one 4,7-phen moiety in **2** by L (pathway *c* in Scheme 1); (iii) by reaction of species **1** and **2** in the proper stoichiometry (pathway *d* Scheme 1 and Fig. 1). Additionally, **3a** can also be obtained by disproportion of **4a** (see below and pathway *f* in Scheme 1).

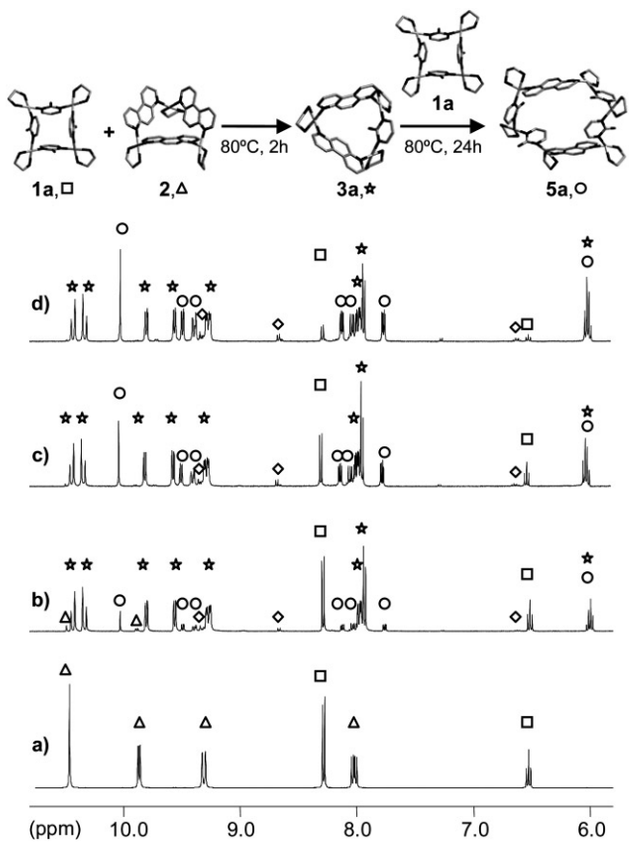

Fig. 1 Evolution, at 80 °C, of a 3 : 4 reaction mixture of homotopic $[Pd(en)(\mu\text{-}N,N'\text{-2-pymo})]_4^{4+}$ (**1a**) and $[Pd(en)(\mu\text{-}N,N'\text{-4,7-phen})]_3^{6+}$ (**2**) followed by ^1H NMR (D_2O, 293 K, 400 MHz). (a) $t = 0$, (b) 2, (c) 5, (d) 24 h. **1a** (squares), **2** (triangles), $[Pd_3(en)_3(\mu\text{-}N,N'\text{-2-pymo})(\mu\text{-}N,N'\text{-4,7-phen})_2]^{5+}$ (**3a**, stars), $[Pd_4(en)_4(\mu\text{-}N,N'\text{-2-pymo})_2(\mu\text{-}N,N'\text{-4,7-phen})_2]^{6+}$ (**4a**, diamonds), $[Pd_6(en)_6(\mu\text{-}N,N'\text{-2-pymo})_4(\mu\text{-}N,N'\text{-4,7-phen})_2]^{8+}$ (**5a**, circles).

The most significant feature on the ^1H NMR spectra of species **3a**, **3b** and **3c** (Fig. 1) is the loss of the original equivalence of the two halves of the 4,7-phenanthroline moieties after ligand exchange of one of them in **2** by L, concomitant to a symmetry lowering from the C_{3v} of **2** to C_s of species **3a** and **3c** and C_1 of **3b**. For instance, in the case of **3a**, the 2-pymo signals are high field shifted, $H_{4,4'}$(−0.30 ppm) and H_5(−0.50 ppm), compared to the parent species **1a**. The 4,7-phen resonances split and shift to high field, $H_{1'}$(−0.02 ppm), H_1(−0.07 ppm), $H_{2,2'}$(0.0 ppm), $H_{3'}$(−0.10 ppm), H_3(−0.35 ppm), $H_{5'}$(−0.05 ppm) and H_5(−0.15 ppm), compared to the parent homotopic species **2**. 2D NOESY ^1H ^1H NMR spectra were also run in order to investigate the complex structure of these heterotopic metallacalix[3]arenes. The results show exchange peaks between the $H_{4,4'}$ pyrimidine ring resonances and the H_2 and H_3 protons of the shielded half of the 4,7-phenanthroline, confirming the simultaneous presence of both ligands *N*,*N*′-bridges in each **3** species. The 2D spectra also prompt for an asymmetric distribution of the 4,7-phen electron density, the latter being more pronounced toward the basic 2-pymo ligand than toward the side close to the other, electron withdrawing, 4,7-phen. In addition, the shielding of pyrimidine ring resonances, compared to those of the 1,3-alternate homotopic species **1**, and the observed exchange peaks of the NOE experiments suggest, for species **3**, a rigid cone conformation.

Suitable single crystals for conventional X-ray diffractometry were obtained for **3c**, unequivocally confirming that it consists of cyclic trinuclear $[Pd_3(en)_3(\mu\text{-}N,N'\text{-4,6-dimethyl-2-pymo})(\mu\text{-}N,N'\text{-4,7-phen})_2]^{5+}$ cations (Fig. 2), nitrate counter ions and water molecules. Crystallographic, data collection and refinement details are gathered in Table 1. The three, crystallographically independent metal ions show slightly distorted square planar coordination and are bridged by the organic moieties in the *N*,*N*′-*exo*-bidentate fashion, thus defining a metallacalix[3]arene. The smaller size of the pyrimidinic moiety and of its bite is reflected by a metal geometry substantially different from that of the precursor $[Pd_3(en)_3(\mu\text{-}N,N'\text{-4,7-phenanthroline})_3]^{6+}$ (**2**) reported by Yu *et al.*[6] Actually, in **2**, the three palladium atoms define an almost equilateral triangle with edges of 7.64 and 7.69 Å,[6] whereas in **3c** they describe an almost isosceles triangle, with edges of 7.56, 7.60 and 5.71 Å, this resulting in a concomitant smaller opening of the metallacalixarene cavity. Nonetheless, in **3c**, the ligands display a pinched-cone disposition, a conformation which, in principle, could allow inclusion of guest molecules even in the solid. The cationic units stack generating channels running along [1 0 0] (Fig. 3). Unexpectedly, no nitrate anions are hosted by the cationic cavities, all of them being distributed around the channels. At variance, three (ordered) water molecules lie at the entrance of the cavity, which thus must be considered slightly hydrophilic: one forms hydrogen-bonds with two en N atoms (2.92 and 2.99 Å), while the other two interact with each other and with a nitrate group sitting above the cavity. The three water oxygens thus realise the maximum possible number of bonding and non-bonding interactions. The remaining (disordered) water molecules are involved in hydrogen-bond interactions with either each other *or* nitrate groups.

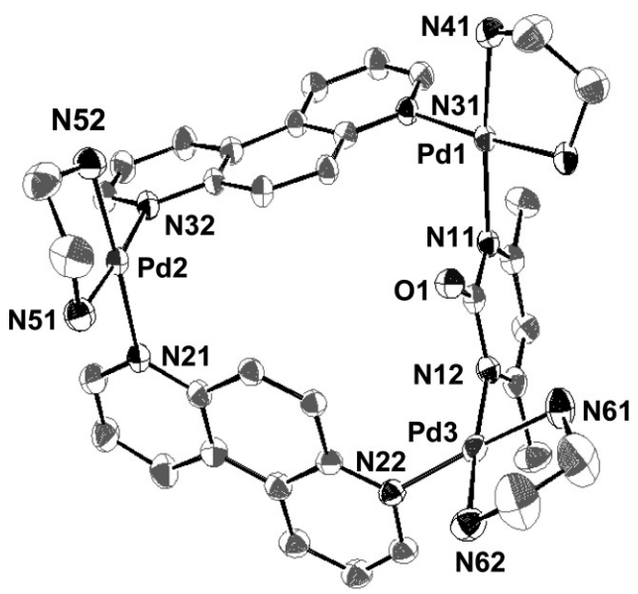

Fig. 2 Ortep representation, at 30% probability, of the metallacalix[3]-arene in $[Pd_3(en)_3(\mu\text{-}N,N'\text{-4,6-dimethyl-2-pymo})(\mu\text{-}N,N'\text{-4,7-phen})_2](NO_3)_5\text{-}(H_2O)_7$, **3c**. Hydrogen atoms omitted for clarity. Significant bond distances (Å) and angles (°) at the metals follow (esds in parentheses): Pd(1)–N(11) 2.038(5), Pd(1)–N(31) 2.056(5), Pd(1)–N(41) 2.027(5), Pd(1)–N(42) 2.023(5), Pd(2)–N(21) 2.036(5), Pd(2)–N(32) 2.046(5), Pd(2)–N(51) 2.023(6), Pd(2)–N(52) 2.012(6), Pd(3)–N(12) 2.052(5), Pd(3)–N(22) 2.059(5), Pd(3)–N(61) 2.017(6), Pd(3)–N(62) 2.028(6); N(11)–Pd(1)–N(31) 92.9(2), N(11)–Pd(1)–N(41) 174.2(2), N(11)–Pd(1)–N(42) 90.4(2), N(31)–Pd(1)–N(41) 91.9(2), N(31)–Pd(1)–N(42) 175.7(2), N(41)–Pd(1)–N(42) 83.8(2), N(21)–Pd(2)–N(32) 89.0(2), N(21)–Pd(2)–N(51) 94.3(2), N(21)–Pd(2)–N(52) 177.0(2), N(32)–Pd(2)–N(51) 176.2(2), N(32)–Pd(2)–N(52) 92.7(2), N(51)–Pd(2)–N(52) 84.0(2) N(12)–Pd(3)–N(22) 92.6(2), N(12)–Pd(3)–N(61) 90.8(2), N(12)–Pd(3)–N(62) 173.9(2), N(22)–Pd(3)–N(61) 176.5(2), N(22)–Pd(3)–N(62) 93.4(2), N(61)–Pd(3)–N(62) 83.2(3).

Tetranuclear species of type $[Pd_4(en)_4(\mu\text{-}N,N'\text{-L})_2(\mu\text{-}N,N'\text{-4,7-phen})_2]^{6+}$ (4)

We have further explored the formation of additional heterotopic polynuclear cyclic species. Our results show that reaction of a 2 : 1 : 1 mixture of ethylenediaminepalladium(II), L and 4,7-phen building blocks leads to the sequential formation of tetranuclear **4** and hexanuclear species **5** (see pathways *e* and *f* in Scheme 1) only for the *unsubstituted* 2-pyrimidinol heterocycle. In contrast to the synthesis of the type **3** species, reaction of homotopic **1a** and **2**

Table 1 Crystallographic data and refinement details for compounds $[Pd_3(en)_3(\mu\text{-}N,N'\text{-}4,6\text{-dimethyl-2-pymo})(\mu\text{-}N,N'\text{-}4,7\text{-phen})_2](NO_3)_5(H_2O)_7$, **3c**, and $[Pd_4(en)_4(\mu\text{-}N,N'\text{-}2\text{-pymo})_2(\mu\text{-}N,N'\text{-}4,7\text{-phen})_2](NO_3)_6{\cdot}H_2O$, **4a**

	3c	**4a**
Empirical formula	$C_{36}H_{61}N_{17}O_{23}Pd_3$	$C_{40}H_{56}N_{22}O_{21}Pd_4$
Formula weight/g mol^{-1}	1419.2	1606.7
Crystallographic system	Triclinic	Monoclinic
Space group	$P\bar{1}$	$C2/c$
a/Å	9.307(3)	28.183(3)
b/Å	15.464(5)	17.702(2)
c/Å	19.806(7)	11.992(1)
α/°	94.337(2)	90.0
β/°	94.914(2)	111.05(1)
γ/°	106.446(2)	90.0
Z	2	4
μ/mm^{-1}	1.08	1.36
Temperature/K	298(2)	298(2)
Measured reflections	26280	18698
Unique reflections	9518	3664
R_{int}, R_σ [a]	0.018, 0.020	0.099, 0.072
$R(F)$ and $wR(F^2)$, for $I > 2\sigma(I)$ [c]	0.055, 0.175	0.047, 0.102
$R(F)$ and $wR(F^2)$, for all data [c]	0.059, 0.182	0.088, 0.120

[a] $R_{int} = \sum|F_o^2 - F_{mean}^2|/\sum|F_o^2|$; $R_\omega = \sum|\sigma(F_o^2)|/\sum|F_o^2|$. [b] $S(F^2) = [\sum w(F_o^2 - F_c^2)^2/(n-p)]^{1/2}$ where n is the number of reflections, p the number of parameters and $w = 1/[\sigma^2(F_o^2) + (0.019P)^2 + 1.88P]$ with $P = (F_o^2 + 2F_c^2)/3$. [c] $R(F) = \sum||F_o| - |F_c||/\sum|F_o|$ and $wR(F^2) = [\sum w(F_o^2 - F_c^2)^2/\sum wF_o^4]^{1/2}$.

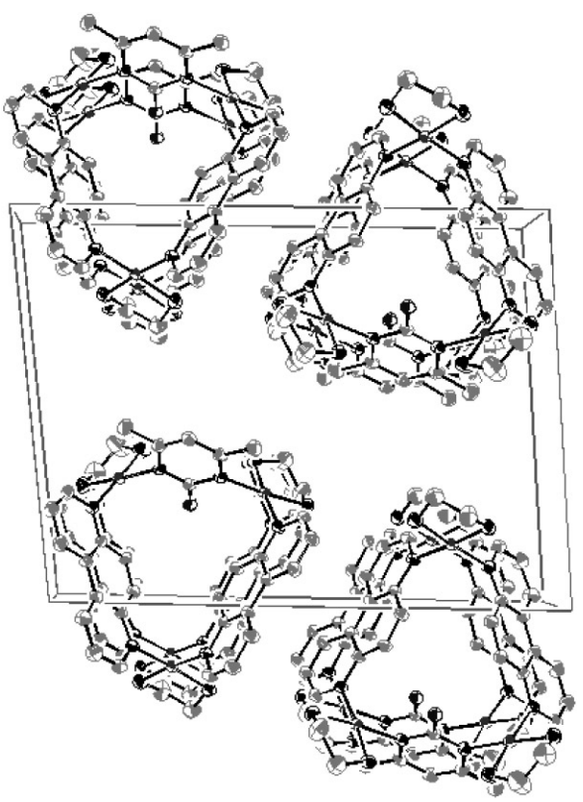

Fig. 3 Ortep representation, at 30% probability, of the packing motif in $[Pd_3(en)_3(\mu\text{-}N,N'\text{-}4,6\text{-dimethyl-2-pymo})(\mu\text{-}N,N'\text{-}4,7\text{-phen})_2](NO_3)_5(H_2O)_7$, **3c**, as viewed down [1 0 0]. Hydrogen atoms, nitrate anions and water molecules omitted for clarity.

metallacalixarenes in the proper stoichiometry (3 : 4) only leads to the formation of a minimum amount of **4a** (Fig. 1).

The ^{1}H NMR studies agree with the formation of the heterotopic tetranuclear species $[Pd_4(en)_4(\mu\text{-}N,N'\text{-}2\text{-pyrimidinolate})_2(\mu\text{-}N,N'\text{-}4,7\text{-phenanthroline})_2]^{6+}$ (**4a**) by direct reaction of the building blocks in a 2 : 1 : 1 ratio (Fig. 4). It should be noted, however, that the attempts to obtain the related **4b** and **4c** species containing the methylated derivatives of 2-pymo were fruitless. For instance, reaction of a mixture of species **1c** and **2**, in the proper stoichiometry, leads to formation of the trinuclear species **3c** in addition to an excess of unreacted **1c**.

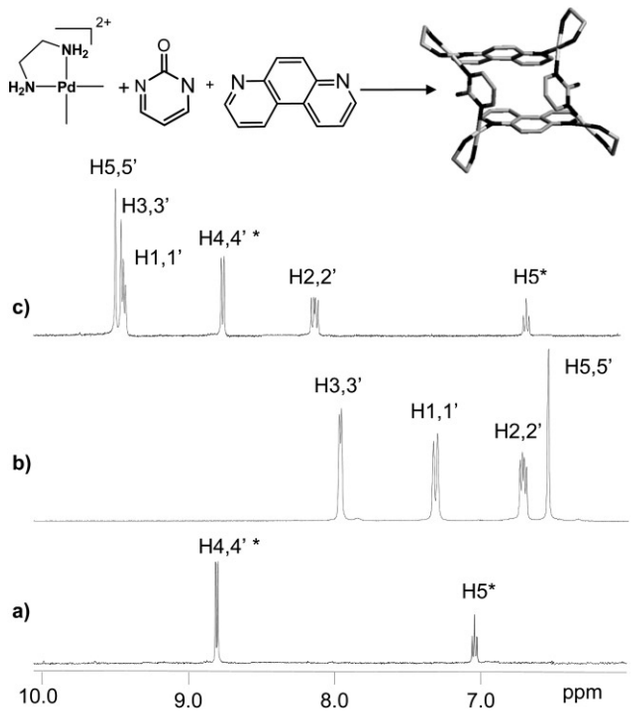

Fig. 4 Schematic reaction between the entries ethylenediamine-palladium(II), 4,7-phen and 2-pymo to give heterotopic $[Pd_4(en)_4(\mu\text{-}N,N'\text{-}2\text{-pymo})_2(\mu\text{-}N,N'\text{-}4,7\text{-phen})_2]^{8+}$ (**4a**) as a single product (above). ^{1}H NMR spectra of (a) H_2pymo^+, (b) free 4,7-phen and (c) $[Pd_4(en)_4(\mu\text{-}N,N'\text{-}2\text{-pymo})_2(\mu\text{-}N,N'\text{-}4,7\text{-phen})_2]^{8+}$ (**4a**). Asterisks denote the pymo resonances. The high down field shift of the 4,7-phen H5,5′ resonances upon metal coordination should be highlighted (see ref. 8).

The most significant feature on the ^{1}H NMR spectra of species **4a** is that the original equivalence of the two halves of both the 4,7-phen and 2-pymo moieties are maintained (Fig. 4), in contrast to what was previously observed for **3a** (see above). In addition, the 2-pymo signals are down field shifted, $H_{4,4'}$ (+0.43 ppm) and H_5 (+0.05 ppm), compared to the parent species **1a**, whereas the 4,7-phen resonances are shifted, $H_{1,1'}$ (+0.10 ppm), $H_{2,2'}$ (+0.20 ppm), $H_{3,3'}$ (−0.40 ppm) and $H_{5,5'}$ (0 ppm), compared to the parent homotopic species **2**. The down field shift of the 2-pymo resonances, compared to the homotopic species **1**, can be related to the length of the 4,7-phen bridges preventing any stacking interaction between the two 2-pymo, to a 1,3-alternate conformation of the bridging ligands and to the electron withdrawing nature of the 4,7-phen bridges. 2D NOESY ^{1}H ^{1}H NMR spectra were also run in order to investigate the complex structure of this heterotopic metallacalix[4]arene. The results show exchange peaks between the 4,7-phenanthroline $H_{2,2'}$, $H_{3,3'}$ and $H_{5,5'}$ resonances and the pyrimidine $H_{4,4'}$ ones, as happens of spatial contacts between the adjacent heterocycles in a conformationally flexible species. Thus, at variance with **3a** (see above), **4a** possesses a conformationally flexible nature similar to that of the parent $[Pd_4(en)_4(\mu\text{-}N,N'\text{-}2\text{-pymo})_4]^{4+}$ (**1a**) species.[9d]

The nature of **4a** has been definitely established by conventional single crystal X-ray diffractometry: pertinent crystallographic, data collection and refinement details are gathered in Table 1. **4a** consists of cyclic $[Pd_4(en)_4(\mu\text{-}N,N'\text{-}2\text{-pymo})_2(\mu\text{-}N,N'\text{-}4,7\text{-phen})_2]^{6+}$ units (Fig. 5), of crystallographic C_2 symmetry, nitrate counter ions and water molecules. The two independent metal ions show slightly distorted square planar coordination, while both independent 2-pymo and 4,7-phen ligands act, as in **3c**, in the *N,N′-exo*-bidentate bridging mode. In the tetranuclear cations, the pyrimidine and phenanthroline moieties alternate along the metallamacrocycle. Yet, quite unexpectedly, the metal ions lie at the vertices of a *parallelogram*, rather than at those of a rectangle. Moreover, the metallacalix[4]arene exhibits a 1,3-alternate conformation, which results in a cavity markedly too small to allow guest molecules inclusion in the solid: indeed, apertures are present of 3.76 Å on the side of 2-pymo ligands (defined as the shortest C···C contact) and of 4.04 Å for the 4,7-phenanthroline ones (defined as the average value

among the shortest C···C contacts). The geometry of the tetranuclear species **4a** can be compared to that of the parent $[Pd_4(en)_4(\mu\text{-}N,N'\text{-}2\text{-pymo})_4]^{4+}$ one (**1**),[9d] showing as well a 1,3-alternate conformation, with the palladium atoms defining a nearly regular square with edges of about 5.9 Å; at variance, in **4a**, due to the different size of 2-pymo and 4,7-phen bridges, two markedly distinct edges are present [5.81 and 7.60 Å]. The cationic units pack in such a way to create a wavy motif about [1 0 0] and columnar entities about [0 1 0] (Fig. 6). In this case, neither nitrate anions nor water molecules occupy the cationic cavities, even if the independent water molecule is located in the vicinity of the metallacalix[4]arene, thus making a hydrogen-bond with an ethylenediamine N atom (3.06 Å). The latter interaction, together with a further hydrogen-bond with a nearby nitrate, grants the water oxygen its maximum number of bonding and non-bonding interactions.

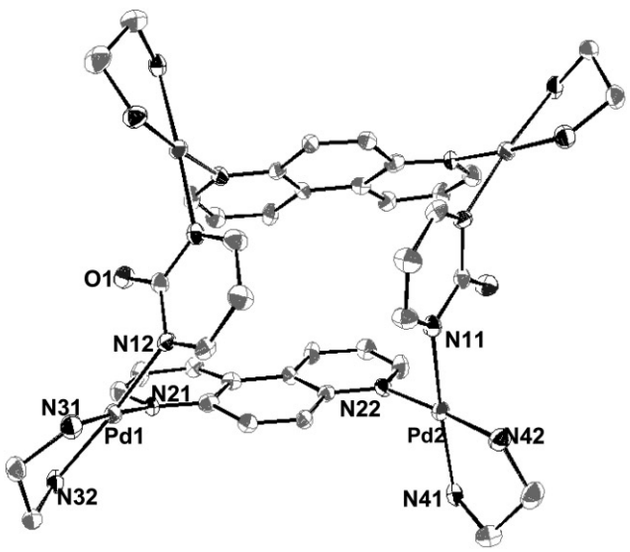

Fig. 5 Ortep representation, at 30% probability, of the metallacalix[4]-arene in $[Pd_4(en)_4(\mu\text{-}N,N'\text{-}2\text{-pymo})_2(\mu\text{-}N,N'\text{-}4,7\text{-phen})_2](NO_3)_6{\cdot}H_2O$, **4a**. Hydrogen atoms omitted for clarity. Significant bond distances (Å) and angles (°) at the metals follow (esds in parentheses): Pd(1)–N(12) 2.037(7), Pd(1)–N(21) 2.047(7), Pd(1)–N(31) 2.022(7), Pd(1)–N(32) 2.028(7), Pd(2)–N(11) 2.034(7), Pd(2)–N(22) 2.044(7), Pd(2)–N(41) 2.014(8), Pd(2)–N(42) 2.003(7), N(12)–Pd(1)–N(21) 90.6(3), N(12)–Pd(1)–N(31) 91.5(3), N(12)–Pd(1)–N(32) 174.2(3), N(21)–Pd(1)–N(31) 177.3(3), N(21)–Pd(1)–N(32) 94.6(3), N(31)–Pd(1)–N(32) 83.4(3), N(11)–Pd(2)–N(22) 92.2(3), N(11)–Pd(2)–N(41) 173.7(3), N(11)–Pd(2)–N(42) 90.4(3), N(22)–Pd(2)–N(41) 94.2(3), N(22)–Pd(2)–N(42) 177.2(3), N(41)–Pd(2)–N(42) 177.2(3).

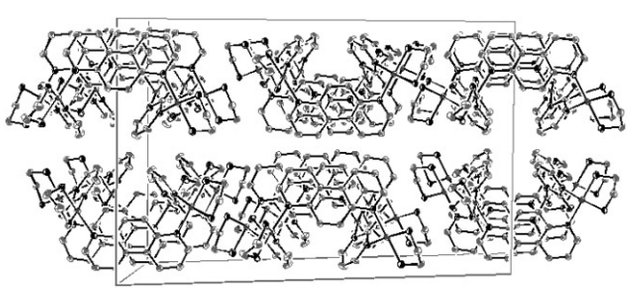

Fig. 6 Ortep representation, at 30% probability, of the packing motif in $[Pd_4(en)_4(\mu\text{-}N,N'\text{-}2\text{-pymo})_2(\mu\text{-}N,N'\text{-}4,7\text{-phen})_2](NO_3)_6{\cdot}H_2O$, **4a**, as viewed down [0 0 1]. Hydrogen atoms, nitrate anions and water molecules omitted for clarity.

It should be noted that species **4a** is not thermodynamically stable, in solution, for a long time. The ^{1}H NMR studies reveal that it disproportionates, after 10 days in solution at room temperature, into a 1 : 2 mixture of a novel hexanuclear species of type $[Pd_6(en)_6(\mu\text{-}N,N'\text{-}2\text{-pyrimidinolate})_4(\mu\text{-}N,N'\text{-}4,7\text{-phenanthroline})_2]^{8+}$ (**5a**) and the previously mentioned trinuclear species $[Pd_3(en)_3(\mu\text{-}N,N'\text{-}2\text{-pyrimidinolate})(\mu\text{-}N,N'\text{-}4,7\text{-phenanthroline})_2]^{5+}$ (**3a**) (see pathway *f* in Scheme 1). The disproportion reaction time can be shortened to *ca.* 24 h when the **4a** solution is heated at 80 °C. Roughly speaking, this would imply an activation energy of *ca.* 40 kJ mol^{-1}. Additionally, **5a** can also be obtained from a 3 : 4 reaction mixture of the homotopic species **1a** and **2**, which shows the sequential formation of heterotopic **3a** (after 2 h of reaction at 80 °C) and the subsequent reaction of the latter with unreacted **1a** to give **5a** (after 24 h of reaction at 80 °C) (see Fig. 1).

Hexanuclear species of type $[Pd_6(en)_6(\mu\text{-}N,N'\text{-}L)_4(\mu\text{-}N,N'\text{-}4,7\text{-phen})_2]^{8+}$ (5)

Species **5a** has been characterised in solution by 1D ^{1}H NMR and 2D NOESY ^{1}H ^{1}H NMR spectra. The results agree with the formation of a novel heterotopic species containing ethylenediaminepalladium(II), 2-pyrimidinolate and 4,7-phenanthroline moieties in a 3 : 2 : 1 ratio. The spectra show the loss of the original equivalence of the two halves of the 2-pyrimidinolate ligands and the maintenance of the C_{2v} symmetry for the 4,7-phenanthroline ligands. In addition, the phenanthroline resonances are shifted, $H_{1,1'}$ (+0.11 ppm), $H_{2,2'}$ (+0.15 ppm), $H_{3,3'}$ (−0.30 ppm) and $H_{5,5'}$ (−0.40 ppm), compared to the parent homotopic species **2**, whereas the 2-pyrimidinolate signals are high field shifted H_4 (−0.15 ppm), $H_{4'}$ (−0.52 ppm) and H_5(−0.50 ppm), compared to the parent species **1a**. The NOE experiments show $H_{2,2'}$ (4,7-phen), H_4 (2-pymo) and $H_{3,3'}$(4,7-phen), $H_{4'}$(2-pymo) exchange peaks. The fact that there are exchange peaks between the phenanthroline signals and both sides of pyrimidine ring suggests a folded, conformationally flexible metallacalix[6]arene of type **5** (Scheme 1). This situation is closely related to the one found for the homotopic hexanuclear species $[Pd(1,2\text{-diaminecyclohexane})(N,N'\text{-}4,6\text{-dimethyl-2-pyrimidininolate})]_6^{6+}$, which presents a folded conformationally flexible cyclic structure.[10] A hexanuclear species of type **5** would agree with both the stoichiometry and its flexible nature, which will also imply shielded phenanthroline and pyrimidinol moieties due to extensive intramolecular π–π interactions.

Host–guest chemistry

The tunable nature and size of the cavities of the metallacalix[*n*]-arenes here described prompted us to explore their host–guest chemistry. In this regard, we have previously reported the receptor properties of metallacalix[*n*]arenes towards biorelevant mononucleotide anions[8] showing in some cases enantioselectivity.[10] In this respect, titration of **3c** and **4a** with adenosine-5′-monophosphate (AMP) shows high-field shifts in the ^{1}H NMR spectra of both host and guest resonances, which agrees with partial adenine heterocycle inclusion inside the metallacalix[*n*]arene cavities. It should also be noted that **4a** titration with AMP results in the appearence of broad sets of signals for the AMP resonances, showing the formation of a host–guest assembly with slow guest exchange rate. In this regard, the *ca.* 7.75 Å separation between the bases of the 2-pyrimidinolate residues is optimal for sandwiching the adenine heterocycle. In the case of the interaction of **3c** with AMP, we have a K_{ass} value of 24 M^{-1}, *ca.* three times lower than the one reported by us[8] for the interaction between **2** and AMP, which can be related to the smaller opening of the cavity of **3c**. It should also be noted that, as observed in previous cases, mononucleotide inclusion induces metallacalix[*n*]arene decomposition.[8,10]

The host–guest chemistry of these species is not restricted to anions: actually, we have observed, on the NOE experiments, cross-peaks between the $H_{2,2'}$ (4,7-phen of **4a**) and $H_{4,4'}$ (2-pymo of **1a**) resonances and the $H_{5,5'}$ (2-pymo of **4a**) and $H_{5,5'}$ (2-pymo of **1a**) ones (Fig. 7). This result suggests the formation of a supramolecular association of the type **4a**–**1a** (Fig. 7), in spite of the positive charge of both species. In order to discard that the NOE cross-peaks arise from a dynamic equilibrium between species **4a** and **1a**, we have exposed **4a** to the **1a** inert platinum analogue, $[Pt(en)(\mu\text{-}N,N'\text{-}2\text{-pymo})]_4(NO_3)_4$, and found also NOE cross-peaks between these two species, proving the formation of a supramolecular association of the type **4a**–**1**. The observed cross-peaks agree with intercalation of one of the 2-pymo residues of **1** into the molecular clip formed by the two 2-pymo residues of **4a**.

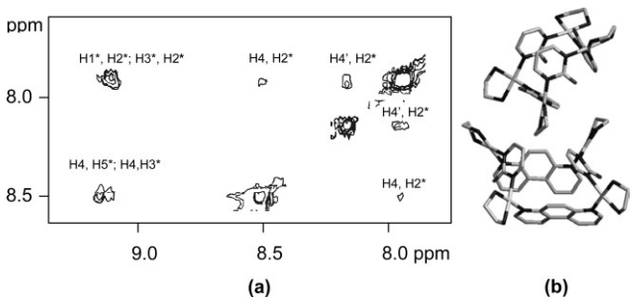

Fig. 7 (a) Section of the 2D 1H 1H NOESY spectrum (D_2O, 293 K, 400 MHz) of a solution containing **4a** and **1a**, showing the cross peaks between the $H_{4'}$ (2-pymo) resonances of the homotopic palladium square and the H_2* (4,7-phen) ones of the heterotopic **4a** parallelogram, which are indicative of an association of both species in solution. Asterisk denotes (4,7-phen) resonances of **4a**. The 2-pymo resonances of **1a** are denoted with primes. (b) Proposed **4a**–**1a** assembly.

Conclusions

In spite of the different nature of 2-pyrimidinolate derivatives and 4,7-phenanthroline bridging ligands, the results presented above prove that the heterotopic cyclic species are favoured over the homotopic ones, which might be related to entropic and statistical reasons as well. Steric factors play also an important role, favouring a specific product from the wide variety of possible ones. Moreover, the investigated reactions proceed almost quantitatively, thus suggesting also an enthalpic driving force. In conclusion, we have shown the possibilities of this strategy for tuning the nature and size of metallamacrocycles cavities for possible selective receptor purposes.

Experimental

$[Pd(en)(N,N'\text{-L})]_4(NO_3)_4$ with L = 2-pyrimidinolate (**1a**), 4-methyl-2-pyrimidinolate (**1b**), 4,6-dimethyl-2-pyrimidinolate (**1c**)[9d,e] and $[Pd_3(en)_3(N,N'\text{-4,7-phen})_3](NO_3)_6$ (**2**)[6] were prepared according to literature methods. 2-pyrimidinol·HCl (2-Hpymo·HCl), 4-methyl-2-pyrimidinol·HCl (2-Hmpymo·HCl), purchased from Aldrich, were converted to the corresponding HNO_3 adducts by anion exchange in a type 3 ion-exchange resine (Merck) in the nitrate form. 4,6-Dimethyl-2-pyrimidinol (2-Hdmpymo), 4,7-phenanthroline (4,7-phen) and monosodium salts of adenosine 5′-monophosphate (AMP) were used as received.

Preparation of $[Pd_3(en)_3(N,N'\text{-L})(N,N'\text{-4,7-phen})_2](NO_3)_5$ with L = 2-pyrimidinolate (3a), 4-methyl-2-pyrimidinolate (3b), 4,6-dimethyl-2-pyrimidinolate (3c)

$[(en)PdCl_2]$ (0.75 mmol) was suspended in an aqueous solution of $AgNO_3$ (1.5 mmol) in water (25 mL); the suspension was stirred in the dark at 60 °C overnight. The resulting mixture was kept at 4 °C for some minutes before the AgCl precipitate was filtered off.

Afterwards, an aqueous solution (30 mL) containing 4,7-phenanthroline (0.5 mmol) and the corresponding 2-pyrimidinol (0.25 mmol) derivative was added to the filtrate and the pH was adjusted to 7.0 by means of NaOH 1 M. The resulting pale yellow solution was allowed to react at 60 °C for 5 h. Alternatively, the type **3** species can be obtained from a 3 : 8 mixture of homotopic $[Pd(en)(N,N'\text{-L})]_4(NO_3)_4$ and $[Pd(en)(N,N'\text{-4,7-phen})]_3(NO_3)_6$ allowed to react at 80 °C for 2 h. Species **3a** to **3c** were characterized by 1D and 2D ^{1}H NMR experiments, but only **3c** was isolated as a pure material in the solid state. X-ray quality crystals of **3c** were obtained after one week from the mother liquor.

3a. ^{1}H NMR (400 MHz, D_2O, 25 °C, TMA): δ (ppm) = 2.93–3.07 (m, 24H; en), 5.99 (t, $J_{4,5}$ = 5.5 Hz; 1H; H_5 pymo), 7.93 (d, 2H; $H_{4,4'}$ pymo), 7.97 (dd, $J_{1,2}$ = 3.2 Hz, $J_{2,3}$ = 5 Hz; 4H; $H_{2,2'}$ phen), 9.26 (d, 2H; H_1 phen), 9.29 (d, 2H; $H_{1'}$ phen), 9.56 (d, 2H; H_3 phen), 9.8 (d, 2H; $H_{3'}$ phen), 10.34 (d, $J_{5,5'}$ = 9.7 Hz, 2H; H_5 phen), 10.44 (d, 2H; $H_{5'}$ phen).

3b. ^{1}H NMR (400 MHz, D_2O, 25 °C, TMA): δ (ppm) = 2.93–3.07 (m, 24H; en), 6.17 (d, $J_{5,6}$ = 5.8 Hz; 1H; H_5 mpymo), 7.90 (d, 1H; H_6, mpymo), 7.96 (m, 4H; $H_{2,2',2'',2'''}$ phen), 9.28 (d, $J_{1,2}$ = 8.3 Hz, 4H; $H_{1,1',1'',1'''}$ phen), 9.57 (m, 2H; $H_{3,3'}$ phen), 9.75 (d, 1H; $H_{3''}$ phen), 9.84 (d, 1H; $H_{3'''}$ phen), 10.35 (d, $J_{5,5'}$ = 9.6 Hz, 1H; H_5 phen), 10.45 (d, 1H; $H_{5'}$ phen), 10.60 (d, 1H; $H_{5''}$ phen), 10.67 (d, 1H; $H_{5'''}$ phen).

3c. Elemental analysis (%): Calculated for $C_{36}H_{63}N_{17}O_{24}Pd_3$ (1437.3 g mol^{-1}): C 30.09, H 4.42, N 16.58. Found: C 30.19, H 4.47, N 16.60. Yield 60%. ^{1}H NMR (400 MHz, D_2O, 25 °C, TMA): δ (ppm) = 2.9–3.1 (m, 24H; en), 2.87 (s, 6H; CH_3 dmpymo), 6.15 (s, 1H; H_5 dmpymo), 7.82 (dd, $J_{1,2}$ = 8.5 Hz, $J_{2,3}$ = 5,2 Hz; 4H; $H_{2,2'}$ phen), 9.13 (d, 2H; H_1 phen), 9.16 (d, 2H; $H_{1'}$ phen), 9.44 (d, 2H; H_3 phen), 9.69 (d, 2H; $H_{3'}$ phen), 10.43 (d, $J_{5,5'}$ = 9.6 Hz, 2H; H_5 phen), 10.66 ppm (d, 2H; $H_{5'}$ phen). The correspondence between single crystals and (re)crystallisation crude product was confirmed by X-ray powder diffraction.

Preparation of $[Pd_4(en)_4(N,N'\text{-L})_2(N,N'\text{-4,7-phen})_2](NO_3)_6$ with L = 2-pyrimidinolate (4a)

$[(en)PdCl_2]$ (1.5 mmol) was suspended in an aqueous solution of $AgNO_3$ (3 mmol) in water (25 mL), and the suspension was stirred in the dark at 60 °C overnight. The resulting mixture was kept at 4 °C for some minutes before the AgCl precipitate was filtered off.

Afterwards, an aqueous solution (20 mL) containing 4,7-phenanthroline (0.75 mmol) and 2-Hpymo·HNO_3 (0.75 mmol) was added to the filtrate. Posterior adjustment of the pH to 7.0 by means of NaOH 1 M and reaction at 80 °C for 24 h affords **4a** quantitatively (^{1}H NMR). Concentration of the solution to 10 mL in the rotavapor at 60 °C gives, after seven days, crystals suitable for X-ray analysis. Elemental analysis (%): Calculated for $C_{40}H_{64}N_{22}O_{25}Pd_4$ (1678.76 g mol^{-1}): C 28.62, H 3.84, N 18.35. Found: C 28.25, H 3.86, N 18.82. Yield 80%. ^{1}H NMR (400 MHz, D_2O, 25 °C, TMA): δ (ppm) = 2.8–3.0 (m, 32H; en), 6.5 (t, $J_{4,5}$ = 5.6 Hz; 2H, H_5 pymo), 7.9 (dd, $J_{1,2}$ = 8.5 Hz, $J_{2,3}$ = 5.6 Hz; 4H; $H_{2,2'}$ phen), 8.50 (d, 4H; $H_{4,4'}$ pymo), 9.19–9.22 (m, 8H; $H_{1,1'}$, $H_{3,3'}$ phen), 9.26 (s, 4H; $H_{5,5'}$ phen). The correspondence between single crystals and (re)crystallisation crude product was confirmed by X-ray powder diffraction.

Preparation of $[Pd_6(en)_6(N,N'\text{-L})_4(N,N'\text{-4,7-phen})_2]^{8+}$ with L = 2-pyrimidinolate (5a)

5a was obtained from a 3 : 4 mixture of homotopic species **1** and **2** which was allowed to react at 80 °C for 24 h. Species **5a** was characterized by 1D and 2D ^{1}H NMR experiments. Alternatively, this species can be obtained from heating **4** for 24 h at 80 °C, giving a 2 : 1 mixture of **3a** and **5a**. Attempts to obtain **5a** as a pure material in the solid phase were fruitless.

5a. ^{1}H NMR (400 MHz, D_2O, 25 °C, TMA): δ (ppm) = 2.95–3.05 (m, 48H; en), 6.00 (t, $J_{4,4'}$ = 5.5 Hz, $J_{4,5}$ = 2.4 Hz; 4H; H_5 pymo), 7.75 (dd, 4H; H_4 pymo), 8.02 (m, $J_{1,2}$ = 8.3 Hz, $J_{2,3}$ = 5.0 Hz; 4H; $H_{2,2'}$ phen), 8.12 (dd, 4H; $H_{4'}$ pymo), 9.39 (d, 4H; $H_{1,1'}$ phen), 9.29 (d, 4H; $H_{3,3'}$ phen), 10.03 (s, 4H; $H_{5,5'}$ phen).

^{1}H NMR experiments

The ^{1}H NMR experiments were recorded in D_2O on a Bruker ARX 400 instrument with tetramethylammonium tetrafluoroborate (TMA) as internal reference (3.18 ppm relative to TMS). 2D NOESY spectra were recorded at 296 K with mixing times in the range between 300 and 1500 ms with a total of 256 t_1 increments, each with 2048 t_2 complex points, were collected with each FID as the average of 32 or 24 transients.

^{1}H NMR titrations

^{1}H NMR experiments carried out for studying the interaction between metallacalix[*n*]arenes and adenosinemonophosphate were performed in D_2O solutions at pD 7.1 in a 5 mm NMR tube

on a BRUKER ARX 400 (400 MHz) instrument with 2.5 mM metallacalix[*n*]arene concentration. ^{1}H NMR spectra were recorded for 10 different mixtures of increasing quantities of solid mono-sodium mononucleotide salts and the shifts of the phenanthroline $H_{1,1'}$ resonances were analyzed using a non linear least-squares method to determine the association constants K_{ass} value.[12]

X-ray crystallography

For both **3c** and **4a**, suitable colourless prisms were mounted in air on the glass fibre tip of a goniometer head. Data collections were performed on a Bruker AXS SMART CCD area-detector equipped with graphite-monochromatised Mo Kα radiation (λ = 0.71073 Å), by applying the ω-scan method with $\Delta\omega = 0.3°$. For **3c**, 2400 frames were acquired with t = 25 s per frame and sample-detector distance fixed at 4.89 cm. Data reduction within the hemisphere with $2\theta < 50.1°$ afforded 26280 reflections, of which 9518 unique. For **4a**, 1860 frames were acquired with t = 30 s per frame and sample-detector distance fixed at 3.88 cm. Data reduction within the hemisphere with $2\theta < 45.1°$ afforded 19053 reflections, of which 3664 unique. An empirical absorption correction was applied in both cases.[13] The structures were solved by direct methods[14] and refined with full-matrix least squares calculations on F^2.[15] Anisotropic temperature factors were assigned to all atoms but (i) hydrogen atoms, riding their parent atoms with an isotropic temperature factor arbitrarily chosen as 1.2 times that of the parent itself, (ii) all water oxygens and (iii) disordered nitrates. Indeed, due to the presence of disorder heavily affecting both some water molecules and some nitrate groups, the two kinds of oxygens were assigned, each, a common isotropic temperature factor. Moreover, to convey further stability during the refinement stage, nitrate bond lengths and angles were restrained according to literature values (N–O 1.25 Å, O–N–O 120°). In the case of **3c**, (i) the five independent nitrate groups have been modeled as three ordered NO_3^-s and three disordered NO_3^-s with sofs adding up to two; (ii) the seven independent water molecules have been described as three ordered H_2Os and ten disordered H_2Os with sofs adding up to four. In the case of **4a**, the four independent nitrate groups have been modeled as two ordered NO_3^-s and three disordered NO_3^-s with sofs adding up to two. Water oxygen positions are substantiated by the presence of hydrogen-bond interactions.

CCDC reference numbers 236530, 236531.

See http://www.rsc.org/suppdata/dt/b4/b408698h/ for crystallographic data in CIF or other electronic format.

Acknowledgements

This work was supported by the Spanish Ministery of Science and Technology through Project: BQU2001-2955-CO2-01 and the 'Acción Integrada Hispano-Italiana': HI2003-0081). SG deeply thanks professors A. Sironi and N. Masciocchi for their help. JARN thanks Johnson Matthey for a generous loan of $PdCl_2$.

References

1 For discrete metal directed assemblies see *e.g.* (*a*) Supramolecular Chemistry and Self-Assembly, a special issue of *Proc. Natl. Acad. Sci. USA*, 2002, **99**(8); (*b*) D. L. Caulder and K. N. Raymond, *Acc. Chem. Res.*, 1999, **32**, 975–982; (*c*) R. H. Fish, *Coord. Chem. Rev.*, 1999, **186**, 569–584; (*d*) S. Lenninger, B. Olenyuk and P. J. Stang, *Chem. Rev.*, 2000, **100**, 853–907; (*e*) J. A. R. Navarro and B. Lippert, *Coord. Chem. Rev.*, 2001, **222**, 219–250; (*f*) R. W. Saalfrank, E. Uller, D. Demleitner and I. Bernt, *Struct. Bonding (Berlin)*, 2000, **96**, 149–176; (*g*) A. Houlton, A. E. Gibson, M. A. Shipman and C. Price, *Chem. Eur. J.*, 2000, **6**, 4371–4378; (*h*) B. J. Holliday and C. A. Mirkin, *Angew. Chem., Int. Ed.*, 2001, **40**, 2022–2043; (*i*) J. J. Bodwin, A. D. Cutland, R. G. Malkani and V. L. Pecoraro, *Coord. Chem. Rev.*, 2001, **216**, 489–512; (*j*) K. Sverin, *Coord. Chem. Rev.*, 2003, **245**, 3–10; (*k*) F. Würthner, C.-C. Yu and C. R. Saha-Möller, *Chem. Soc. Rev.*, 2004, **33**, 133–146.

2 For extended metal organic frameworks see *e.g.* (*a*) O. M. Yaghi, M. O'Keeffe, N. W. Ockwig, H. K. Chae, M. Eddaoudi and J. Kim, *Nature*, 2003, **423**, 705–714; (*b*) C. Janiak, *Dalton Trans.*, 2003, 2781–2804; (*c*) S. L. James, *Chem. Soc. Rev.*, 2003, **32**, 276–288; (*d*) S. Kitagawa, R. Kitaura and S. Noro, *Angew. Chem., Int. Ed.*, 2004, **43**, 2334–2375.

3 (*a*) Y. Kubota, S. Sakamoto, K. Yamaguchi and M. Fujita, *Proc. Natl. Acad. Sci. USA*, 2002, **99**, 4854–4856; (*b*) D. Fiedler, D. H. Leung, R. G. Bergman and K. N. Raymond, *J. Am. Chem. Soc.*, 2004, **126**, 3674–3675; (*c*) M. Albrecht, *J. Inclusion Phenom.*, 2000, **36**, 127–151; (*d*) R. Vilar, *Angew. Chem., Int. Ed.*, 2003, **42**, 1460–1477.

4 (*a*) Z. Grote, R. Scopelliti and K. Sverin, *Angew. Chem., Int. Ed.*, 2003, **42**, 3821–3825; (*b*) J. R. Nitschke and J. M. Lehn, *Proc. Natl. Acad. Sci. USA*, 2003, **100**, 11970–11974.

5 (*a*) T. Kusukawa and M. Fujita, *J. Am. Chem. Soc.*, 1999, **121**, 1397–1398; (*b*) M. Yoshizawa, T. Kusukawa, M. Fujita and K. Yamaguchi, *J. Am. Chem. Soc.*, 2000, **122**, 6311–6312; (*c*) M. Yoshizawa, Y. Takeyama, T. Kusukawa and M. Fujita, *Angew. Chem., Int. Ed.*, 2002, **41**, 1347–1409.

6 S. Y. Yu, H. Huang, H. B. Liu, Z. N. Chen, R. B. Zhang and M. Fujita, *Angew. Chem., Int. Ed.*, 2003, **42**, 686–690.

7 (*a*) H. Chen, S. Ogo and R. H. Fish, *J. Am. Chem. Soc.*, 1996, **118**, 4993–5001; (*b*) Z. Q. Qin, M. C. Jennings and R. J. Puddephatt, *Inorg. Chem.*, 2002, **41**, 3967–3974; (*c*) H. Piotrowski, K. Polborn, G. Hilt and K. Sverin, *J. Am. Chem. Soc.*, 2001, **123**, 2699–2700; (*d*) M. J. Rauterkraus and B. Krebs, *Angew. Chem., Int. Ed.*, 2003, **43**, 1300–1303.

8 M. A. Galindo, J. A. R. Navarro and M. A. Romero, *Dalton Trans.*, 2004, 1563–1566.

9 (*a*) H. Rauter, E. C. Hillgeris, A. Erxleben and B. Lippert, *J. Am. Chem. Soc.*, 1994, **116**, 616–624; (*b*) J. A. R. Navarro, M. B. L. Janik, E. Freisinger and B. Lippert, *Inorg. Chem.*, 1999, **38**, 426–432; (*c*) J. A. R. Navarro, E. Freisinger and B. Lippert, *Eur. J. Inorg. Chem.*, 2000, 147–151; (*d*) J. A. R. Navarro, E. Freisinger and B. Lippert, *Inorg. Chem.*, 2000, **39**, 2301–2305; (*e*) J. A. R. Navarro and J. M. Salas, *Chem. Commun.*, 2000, 235–236.

10 E. Barea, J. A. R. Navarro, J. M. Salas, M. Quirós, M. Willermann and B. Lippert, *Chem. Eur. J.*, 2003, **9**, 4414–4421.

11 K. Yamanari, S. Yamamoto, R. Ito, Y. Kushi, A. Fuyuhiro, N. Kubota, T. Fukuo and R. Arakawa, *Angew. Chem., Int. Ed.*, 2001, **40**, 2268–2271.

12 H. Sigel, K. H. Scheller, V. M. Rheinberger and B. E. Fischer, *J. Chem. Soc., Dalton Trans.*, 1980, 1022–1028.

13 G. M. Sheldrick, *SADABS, Program for area detector adsorption correction*, Institute for Inorganic Chemistry, University of Göttingen, Germany, 1996.

14 A. Altomare, M. C. Burla, M. Camalli, G. L. Cascarano, C. Giacovazzo, A. Guagliardi, A. G. G. Moliterni, G. Polidori and R. Spagna, *J. Appl. Crystallogr.*, 1999, **32**, 115; *SIR97: package for structure solution by direct methods*, A. Altomare, G. Cascarano, C. Giacovazzo, A. Guagliardi, A. G. G. Moliterni, M. C. Burla, G. Polidori, M. Camalli, R. Spagna, University of Bari, Bari, Italy, 1997.

15 G. M. Sheldrick, *SHELX-97, Program for refinement of crystal structures*, University of Göttingen, Germany, 1997.